Iñañez, J.G., Bettencourt, J., Coelho, I.P. et al. *Hit and sunk: provenance and alterations of ceramics from seventeenth century Angra D shipwreck*. **Archaeol Anthropol Sci** 12, 182 (2020). This version of the article has been accepted for publication, after peer review (when applicable) and is subject to Springer Nature's AM terms of use, but is not the Version of Record and does not reflect post-acceptance improvements, or any corrections. The Version of Record is available online at: https://doi.org/10.1007/s12520-020-01109-y

Hit and sunk: provenance and alterations of ceramics from 17th century Angra D shipwreck

J. G. Iñañez[1*], J. Bettencourt[2], I. Pinto Coelho[2], A. Teixeira[2], . G. Arana[3], K. Castro[3], U. Sanchez-Garmendia[1,3],

[1]GPAC, Geography, Prehistory and Archaeology Dpt., University of the Basque Country (UPV/EHU), C.I. Micaela Portilla, c/ Justo Vélez de Elorriaga, 1, 01006 Vitoria-Gasteiz (Spain) (javier.inanez@ehu.eus; uxue.sanchez@ehu.eus)
[2] Faculdade de Ciências Sociais e Humanas - Universidade Nova de Lisboa; CHAM - FCSH/UNL e UAç, Avenida de Berna, 26-C, 1069-061 Lisboa (jbettencourt.cham@gmail.com; texa@fcsh.unl.pt; inespintocoelho@fcsh.unl.pt)
[3]IBeA, Analytical Chemistry Dpt, University of the Basque Country (UPV/EHU), Leioa, Barrio Sarriena s/n 48940, Leioa (Spain) (gorka.arana@ehu.eus; kepa.castro@ehu.eus)

*corresponding author: GPAC, Geography, Prehistory and Archaeology Dpt., University of the Basque Country (UPV/EHU), Centro Investigación Micaela Portilla, c/ Justo Vélez de Elorriaga, 1, 01006 Vitoria-Gasteiz (Spain) (javier.inanez@ehu.eus), tlf. +34-945014549
ORCID: 0000-0002-1411-8099

FINAL DRAFT

PUBLISHED ARTICLE: DOI: 10.1007/s12520-020-01109-y

Archaeological and Anthropological Sciences, 12:182, 2020, pp. 1-16

Springer Nature SharedIt initiative:

https://rdcu.be/b5LDc

Abstract

A set of 34 archaeological ceramics, including olive jars, transparent green lead glazed, tin-lead glazed and unglazed ceramics, from 17th century Angra D shipwreck found at Terceira Island (Azores Archipelago, Portugal) was archaeometrically characterized by Inductively Coupled Plasma Mass Spectrometry (ICP-MS), X-ray Diffraction (XRD) and Scanning Electron Microscopy (SEM). Ceramic provenance has been established by statistical exploration of the ICP-MS chemical data, suggesting as being mainly from Seville origin (southern Spain) and, at a lesser extent, from the north of Portugal, piling up evidences to suggest a Spanish ship. Alteration and contamination effects of underwater environment in calcareous ceramics are assessed by XRD and SEM-EDS analyses, like the crystallization of zeolites, as well as pyrite.

Kewords

Colonial ceramic, Portuguese and Spanish colonialism, archaeometry, shipwreck

1. Introduction

The European expansion determined the crucial role of the Azorean archipelago geographical position. Through the whole 16th and part of the 17th century, the main Atlantic port of call was located on Terceira Island, at Angra, which became a deep sea harbour for Portuguese and Castilian ships returning to Europe (Meneses, 2008, 2005) (Figure 1).

The archaeological record related to this historical background is rich. The first underwater studies with acceptable scientific standards were conducted from 1995 to 2001 and led to the survey of several wrecks (like Angra A and B) and the rescue excavation of two wrecks, Angra C and Angra D (Garcia and Monteiro, 2001; Garcia et al., 1999). In 2006, a new project in Angra bay started, which included the examination of the available data related to Angra D (site geographical coordinates 38°39'09.1"N 27°13'07.1"W). The study of the archaeological context was based on the analysis of field data and in the systematic study of the materials (Bettencourt, 2017).

The ongoing analysis of the artefact distribution has shown that the remains were mostly on the axis of the ship, between or under the ballast, with the greatest concentration near the stern. The fragmentation and the low density of the materials suggest the ship was salvaged, which would have been facilitated by the shallowness and proximity to the shoreline (around 100 m). The presence of modern artefacts indicates the contexts were disturbed by post-depositional processes. However, the ceramic shards assemblage seems to show that some materials did not have very important horizontal displacements. Therefore, we consider that the main ceramic groups are associated with the shipwreck

The ship is an Iberian construction due to the amount of archaeological signatures presented that coincide with the ones proposed by Oertling (2001). The material culture associated with the ship is extensive and varied, including personal possessions and everyday objects or faunal remains (Bettencourt, 2017; García et al., 1999). The ceramics are the largest group and fundamental to understand this archaeological site: statistical analysis shows that olive jars are clearly the most represented group, with over 60% of the total sample (2706 fragments). Red earthenware is also a significant group, with almost 18% (corresponding to 794 fragments), as well as the tin-glazed ware, with around 14% (612 fragments). Lead-glazed ware is a smaller group, with 7% (324 fragments) (Figure 2).

The recognized olive jars - called botijas in the Spanish early-modern written sources - correspond to the middle style typology of Goggin (Goggin, 1960), in a pattern similar to the one recorded on the Tortugas wreck *Atocha* and *Santa Margarita,* salvaged in Florida (1622) (Marken, 1994: 65-71; Avery, 1997: 103-106; Stemm et al., 2013). Besides, two fragments have the mark "IHS" printed, classified as belonging to the Society of Jesus, and another mark consisting of a circular motif accompanied by a serpentine symbol, like the ones recovered in contexts dated between 1610 and 1630 (Bettencourt, 2017, p. 392).

The white plain and the blue on white tin-lead glazed group includes bowls, dishes and chamber pots, very similar to those classified as southern Spanish productions, representing 8% of the total assemblage (360 fragments). The blue on blue tin-lead glazed ceramics are mostly represented by dishes, but we can also identify bowls, summing up less than 3% of the collection (122 fragments);

it is typologically considered as an Andalusian production from mid-16th century to the first quarter of the 17th century. Around a third of the lead-glazed ceramics can also be classified as a Sevillian production (97 fragments), noting that more than a half of these are green glazed basins produced between the end of the 15th and the 17th century. (Deagan, 1987; Marken, 1994).

Unlike olive jars, the other earthenware ceramics are a very heterogeneous group, although it can be broadly framed in Merida Ware Type, including plates, bowls and pots. Although often attributed to Spanish and Portuguese workshops, a set of 135 fragments (3% of the whole assemblage) have clear similarities with 16th and 17th centuries Aveiro productions, with a widespread distribution in the Atlantic space, namely in areas of the Spanish colonization (Bettencourt and Carvalho, 2008). The ceramic assemblage includes some fragments of northern European productions, such as Werra ware (15 fragments) and Rhenish Stoneware (3 fragments), and also Chinese porcelain. The Werra fragments can be dated from the 1st quarter of the 17th century, but the Chinese porcelains belongs to the 2nd half of the 16th century (Bettencourt, 2017, pp. 373-375).

2. Goals

The main goal of this study is shedding light to the historical understanding of the Angra D shipwreck through its ceramic cargo. Importantly, this ship wrecked in the Portuguese harbour of Angra do Heroismo, Terceira Island (Azores Archipelago, and while some evidences pointed out towards a Spanish origin of the ship, its cargo of ceramics remained to be archaeometrically explored. The provenance of the ceramics permits piling up evidences towards establishing the origin of the ship and the maritime route that this ship undertook.

3. Analytical Methodology

A set of 34 archaeological ceramics, including olive jars, tin-lead glazed and unglazed ceramics, was archaeometrically characterized. Among the studied ceramics there are 16 olive jars (*botijas*), 2 red unglazed, 3 transparent green lead glazed, 6 blue on blue tin-lead glazed, 1 blue on white tin-lead glazed, and 6 white plain tin-lead glazed ceramics (Table 1). These ceramics were analyzed by means of Inductively Coupled Plasma Mass Spectrometry (ICP-MS), X-ray

Diffraction (XRD) and Scanning Electron Microscopy (SEM). Analytical methodology is described for each technique as follows:

2.1. Chemical analysis procedure

In the present study, ~10 g of each collected ceramic was powdered using a Herzog HSM 100 pulverizer milling machine equipped with tungsten carbide twin eccentric disks for 30s (HERZOG Automation Corp.). Prior to grinding, glazes and exterior surfaces were mechanically removed by means of a tungsten carbide abrading tool, leaving only the inner part of the ceramic for analysis. This step served to minimize contamination of the ceramic matrix by glaze and soil. Powdered specimens were stored in polyethylene vials for transport to the laboratory.

Sample manipulation and ICP-MS analysis were carried out in a laboratory clean room (class 100). Commercial reagents (Merck Pro Analysis hydrofluoric acid 50.2% and nitric acid 69.8%) were purified by sub-boiling quartz-distillation (HNO_3) and Teflon bottle-distillation (HF). Ultrapure water (resistivity ≥ 18.2 MΩ) was obtained by electrodeionization (Elix Millipore) and polishing by reverse osmosis (Nanopure Barnstead). The flux agent was $LiBO_2$ (Anhydrous, For Analysis Grade Pure) of Corporation Scientifique Claisse, with solution of 50% LiBr (Merck Suprapur) in deionized water used as antiadherent. Certified Reference Materials (CRM) of geological nature were obtained from the Geological Surveys of Japan: andesite JA2, granodiorite JG-1a, granite JG-2, and basalt JB-3. The solutions of unknown samples and Certified Reference Materials for external calibration, validation of the method and preparation of procedural blanks were obtained by alkaline fusion with $LiBO_2$ in Pt–Au crucibles, followed by acid dissolution of the melt. The fusion process was as follows: 250 mg of sample and 500 mg of flux were put into the crucible with three to four drops of LiBr solution as non-wetting agent. The mixture was fused using a Claisse propane fusion instrument (Corporation Scientifique Claisse, Québec, Canada). The melted mixture was poured automatically onto a weighed polypropylene beaker containing 100 mL HNO_3 1N, with a few drops of HF to ensure stability of the HFSE. The acid solution was stirred ca. 10 min to ensure total dissolution. This primary solution was diluted gravimetrically to ca. 1:200 in

a mixture of HNO_3 0.32N and very diluted HF, and spiked with In (50 µg L^{-1}) and Bi (10 µg L^{-1}) standard solutions (García de Madinabeitia et al., 2008).

Chemical element analysis was carried out with a NexION 300 ICP/MS (PerkinElmer, Ontario, Canada), provided with Ryton cross-flow nebulizer, Scott-type double pass spray chamber and standard nickel cones. Argon (99.999%, Praxair, Spain) was used as carrier gas in the ICP/MS measurements. The concentrations of a wide range of analytes ^{27}Al, ^{31}P, ^{88}Sr, ^{120}Sn, ^{90}Zr, ^{93}Nb, ^{133}Cs, ^{137}Ba, ^{139}La, ^{140}Ce, ^{141}Pr, ^{142}Nd, ^{147}Sm, ^{153}Eu, ^{158}Gd, ^{159}Tb, ^{164}Dy, ^{165}Ho, ^{166}Er, ^{169}Tm, ^{174}Tb, ^{175}Lu, ^{180}Hf, ^{181}Ta, $^{206+207+208}Pb$, ^{232}Th and ^{238}U (Internal standards: In and Bi) were analyzed in standard mode; while ^{23}Na, ^{24}Mg, ^{28}Si, ^{39}K, ^{44}Ca, ^{47}Ti,^{51}V,^{52}Cr,^{55}Mn,^{56}Fe,^{59}Co,^{60}Ni, ^{63}Cu and ^{66}Zn (Internal standard: In) were analyzed in collision mode with He as cell gas.

The plasma operating conditions such as the nebulizer flow rate, the position of the torch and the ion lens voltages of the instrument were optimized everyday prior to any experiment with a 10 ng/mL standard solution of Mg, Rh, In, Ba, Pb and U. The nebulizer gas-flow rate at 0.9-1.0 L/min and the plasma gas flow at 18 L/min were optimized to obtain a good compromise between high sensitivity and low oxide levels (lower than 2.5% for CeO/Ce). Sample introduction and experimental conditions for the data acquisition of de ICP-MS per sample were optimized at 20 sweeps, 1 reading and 3 replicates, with an integration time of 1000 ms (see

2.2. Mineralogical procedure

Powder ceramic samples were mineralogical characterized by powder X-ray diffraction (XRD), using a powder diffractometer PANalytical Xpert PRO that incorporates a copper tube (λCuKαmedia = 1.5418 Å, λCuKα1 = 1.54060 Å, λCuKα2 = 1.54439 Å), vertical goniometer (Bragg-Brentano geometry), programmable divergence aperture, automatic interchange of samples, graphite secondary monochromator and PixCel detector.

The measurement conditions were 40 kV of voltage and a current of 40 mA, with an angular range (2θ) scanned between 5 and 70°. Mineral phases present in the samples were identified using X'pert HighScore (PANalytical) software in combination with the powder diffraction file database PDF2 (International Centre for Diffraction Data - ICDD, Pennsylvania, USA).

2.3. Scanning Electron Microscopy procedure

The SEM study was conducted on a fresh fracture (transverse to the wall and parallel to the vertical dimension of the vessel) obtained from each of five pieces, comprising olive jars and tin-lead glazed ware. The samples were gold coated and examined under an EVO 40 Carl-Zeiss SEM coupled to an energy dispersive X-ray analyzer (EDS). Sample examination was conducted at 30kV under full vacuum conditions.

2.4. Statistical approach

The statistical analysis of the data followed Aitchison's approach and Buxeda's observations on compositional data (Aitchison, 2008, 1986; Buxeda i Garrigós and Kilikoglou, 2003; Buxeda i Garrigós, 1999). The statistical procedure consists of the use of ratios of logarithms obtained by dividing all the components, in this case chemical components, by the component that introduces the lowest chemical variability to the entire set of specimens taking into consideration, overcoming the compositional data problem called ''close to unit sum'', when data necessarily must sum 100%. Moreover, the use of logarithms compensates for differences in magnitudes between major elements, such as Al_2O_3 or Fe_2O_3, and trace elements, such as the lanthanide or rare earth elements (e.g. La, Ce, Sm, etc.) and log-transformed data serve to make the distributions of geochemical data more nearly normal. Finally, the log ratio transformation also highlights possible perturbations in the chemical data as a result of diagenesis, contamination, or other alteration processes (see Buxeda i Garrigós, 1999, and Martin-Fernandez et al. 2015 for a thorough discussion on the use of log-ratio principles).

The data were examined using an array of multivariate statistical procedures. The application of multivariate statistical techniques to multielemental chemical data facilitates identification of compositional groups. Therefore, similarity of individuals, and subsequently their hypothetical provenance according to the provenance postulate (Weigand et al., 1977), was tested using Principal Component Analysis. In order to assess the provenance of unknown ceramics from Angra, their chemical fingerprints were compared against well-known archaeometrical reference groups from the main production

centers of the Iberian Peninsula and colonial sites in America (Buxeda i Garrigós et al., 2015; Iñañez et al., 2009, 2008; Sanchez-Garmendia et al., 2019). This database consists of more than 1000 individuals analyzed using multiple analytical techniques: ICP-MS, XRF, AAN, SEM, XRD. Most of the ceramics contained in this database correspond to the main production centers of postmedieval ceramics from the Iberian Peninsula (Seville, Lisbon, Aveiro, Talavera de la Reina, Puente del Arzobispo, Paterna, Manises, Barcelona, Reus, Vilafranca del Penedès, Lleida, Teruel, Muel, Villafeliche, Logroño, Orduña and Elosu), as well as to a multitude of peninsular consumer centers. There is also a number of individuals from the Canary and Azores Islands, as well as a large number of American colonial ceramic materials, especially from Panama, Peru, Colombia, the Dominican Republic and the United States of America, among others.

3. Results and discussion

Although sample preparation was conducted under great care to minimize the analytical error, the potential for contamination exists nonetheless and a conservative approach to data interpretation is warranted. Thus, Co was removed from consideration during the statistical treatment because cobalt is a known binder in the tungsten carbide cell used to grind the samples. Additionally, Ni concentrations were below detection limits for many of the samples and subsequently were removed from consideration. Moreover, Pb and Sn were not used in the statistical treatment since these elements are major components of the glaze composition for tin-lead glazed and green lead glazed wares. In addition, P_2O_5 was also neglected in statistical routines due to its high variability and potential as a key-role element in alteration processes in underwater environments (Lemoine and Picon, 1982; Pradell et al., 1996; Maritan and Mazzoli, 2004).

In addition, previous studies reported the crystallization of new formed zeolites in many calcareous Spanish colonial ceramics (Iñañez, 2007; Iñañez et al., 2009). This process occurs with the leaching of potassium and, sometimes, rubidium, from the matrix, with a subsequent enrichment of sodium because of analcime crystallization (Buxeda i Garrigós et al., 2002; Iñañez et al., 2007; Schwedt et al., 2006). Due to the fact that these alteration and contamination

processes affect those components in the ceramic chemical composition, without any possibility of carrying out a satisfactory correction, Na_2O, K_2O and Rb were removed from consideration during the statistical analysis.

With a view to understand the chemical nature and relationships within the sample under study, a thorough statistical multivariate approach has been conducted. Along these lines, the variability of each chemical component has been taken into account in this study and assessed by calculating the variation matrix using R software (R Core Tema, 2014), which provides information about those components that introduce higher variability to the data set. As has been pointed out by Buxeda i Garrigós (1999) and Buxeda i Garrigós and Kilikoglou (2003), the variation matrix gives a measure of the variability in the covariance structure, defined as total variation (vt). Thus, this number is the measure of the variability existing in the compositional data under study. As a summary of this study, the analysis of the compositional variation matrix shows a total variation of 7.18 (Figure 3), denoting the polygenic characteristics of the chemical compositions of the different paste reference groups and the unknown ceramic shards (Buxeda and Kilikoglou, 2003). The study of the compositional variation matrix has shown that, in addition to the elements already known as problematic due to their relationship with phases of alteration and/or contamination (Na_2O, K_2O and Rb), there is a relatively high variability of other chemical elements used in the first statistical approach. These elements are mainly MgO and Ni, in addition to CaO and Sr. However, CaO and MgO can be considered elements directly related to technology and individual or collective behavioural action by the artisans who manufactured these ceramics, who leave their imprint it (see Buxeda et al., 2008, Skibo and Schiffer, 2008). The elements that can be considered mainly responsible for this variation are MnO, CaO, Pb, Sr, MgO, Ni, P_2O_5, all of them showing a tv/τ.i <0.5, in: contrast, the variable that introduces the least variability into the data set is Nb (tv/τ.i=0.929). However, when not considering the contribution of the elements Pb, Sn, P_2O_5, Co, Ni, Cr, Ta, Zn, Na_2O, K_2O and Rb possibly due to alterations that are difficult to identify by simple chemical analysis or due to the analytical reasons explained above, the variable that introduces the least variability to the set of data consists of Ho (tv/τ.i=0.914), while the total variability is significantly reduced (tv=1.14) (Figure 3). For these

reasons, Ho has been chosen as a divisor in the subsequent transformation into logarithms of ratios.

In order to assign a provenance to the unknown pieces recovered at the site of Angra D, we have undertaken the statistical study of the data set, showing here the reference groups that are historically coherent with the topic since they originate from the main sources of ceramic supply at that time of the Iberian Peninsula: Seville, Manises, Talavera, Barcelona, Gibraltar Strait region (Groups A and B), Lisbon and Aveiro. For this purpose, a main component analysis has been performed. This type of statistical exploration consists of reducing the existing numerical dimensions in the data set by identifying the main variations (principal components analysis or PCA) based on the covariation matrix linear transformation. These new principal components are sorted in order of importance from largest to smallest, with PCA1 accounting for the largest variation over the data set, PCA2 for the second largest variation, and so on. The also transformed compositions of the studied ceramic shards are projected onto this new dimension and their spatial relationships are studied as well, using for comparison purposes the main reference groups from the suitable production centers historically coherent with the subject (e.g. Seville, Manises, Talavera, Muel, Lisbon). Hence, a statistical analysis of main components has been carried out on the sub-composition Al_2O_3, BaO, CaO, Ce, Cr, Cs, Dy, Er, Eu, Fe_2O_3, Gd, Hf, K_2O, La, Lu, MgO, Na_2O, Nb, Nd, Pr, Rb, Si_2O, Sm, Sr, Tb, Th, Ti_2O, Tm, U, V, Yb, Zr with the additive log-ratio transformation using Ho as divisor (Figure 4). The study of the principal components indicates that the first seven principal components account for 95% of the variance of the data set, with the first two principal components explaining a variance of 83.55% of the data set. This allows for a reliable statistical reduction of the n-dimensional reality of the set of elements and samples, as shown by the projection of the analyzed ceramic individuals using the calculated values of the principal components 1 and 2 on the horizontal and vertical axis, respectively.

Following a conservative approach, and in order to avoid overlapping among chemical reference groups with similar chemical fingerprints as a consequence of the high standardization and chemical similarity of the materials and to provide with solid and univocal provenance, unglazed and glazed ceramics discovered at Angra D shipwreck have been studied separately. Thus, Results

are summarized in Figure 4 and 5 for unglazed and glazed wares, respectively. Along these lines, Figure 4 graphically displays the Principal Component Analysis (PCA) regarding unglazed ceramics employing Al_2O_3, BaO, CaO, Ce, Cr, Cs, Dy, Er, Eu, Fe_2O_3, Gd, Hf, La, Lu, MgO, Nb, Nd, Pr, Si_2O, Sm, Sr, Tb, Th, Ti_2O, Tm, U, V, Yb, Zr. Thus, PCA indicated that 90% of the cumulative variance was accounted for in the first 6 principal components, resulting in a good estimation of the overall composition of the ceramic shards. An examination of various projections of the data facilitated the identification of the SEV-A chemical reference groups attributed to Seville as the primary production center responsible for the production of olive jars found in Angra D shipwreck. In fact, all the unglazed ceramics from Angra D fell into this group, with the exception of two unglazed red pots (ANG030 and ANG031). These two unglazed red pots were archaeologicall classified as possible Aveiro ceramics, a northern Portuguese pottery production. These two red ceramics were non-calcareous, while Sevillian ceramics were highly calcareous, and show higher Al content than the Sevillian groups. Additionally, and in order to provide with a solid provenance to these red wares, a sample of 16 ceramics from Ria de Aveiro A shipwreck cargo, produced in the city of Aveiro, was also utilized for comparison purposes (Bettencourt and Carvalho, 2008; Sanchez-Garmendia et al., in press). Therefore, in Figure 4 it is clearly depicted that the provenance of Aveiro for the red ware ceramics found in Angra D shipwreck can be confirmed.

As stated above, and for a better visual group separation purposes, separation of the different types of ceramics (red ware, olive jar, green glazed and tin-lead glazed ceramics) is required. Therefore, in order to obtain a better graphic visualization, tin-lead glazed and green glazed ceramics- have been compared against the main post-medieval glazed and tin-lead glazed production centers from the Iberian Peninsula (Figure 5) (Iñañez et al., 2016; Iñañez et al., 2008; Buxeda et al., 2015; Iñañez 2007). Figure 5 summarizes the statistical study of the chemical differences among productions and unknown ceramics. Thereby, all of the glazed and tin-lead glazed ceramics show high chemical similarity with Sevillian provenance, specifically with SEV-C group. This SEV-C reference group is made out of honey-glazed, transparent green lead glazed and different types of tin-lead glazed ceramics unearthed in production contexts (e.g. kilns, kiln dumps) from the city of Seville (Iñañez 2007; Gomez-Ferrer et al., 2013;

Buxeda et al., 2015; Fernández de Marcos et al., 2017). Interestingly, both transparent green lead glazed and tin-lead glazed show the same provenance, which can suggest that were made using the same paste or clay. Additionally, it can be highlighted that main chemical differences between the two Sevillian groups are mainly due to differences in CaO, MgO and MnO, likely in relation to slight differences in the choice of the clay bed and technological choices made by potters and their guilds (Fernández de Marcos et al., 2017). Chemical groups identified in the Angra D dataset are summarized in Table 2.

The ceramics from Angra D shipwreck according to their ceramic type can be seen in the system SiO_2-Al_2O_3-CaO+Fe_2O_3+MgO (Figure 6). This triangular diagram shows how most of the individuals are located in the quartz-anorthite-wollastonite thermodynamic equilibrium triangle and in the wollastonite-anorthite-mullite triangle. According to that, starting from a hypothetical magma with the composition of these ceramics, their cooling would lead to the crystallization of the above minerals. Of course, in the study of ceramics, one does start from a paste composed of clay minerals and other rock material, which are part of both the clay phase and the non-plastic particles or tempers, not from a magma. As the temperature increases during the firing, the primary mineral phases will begin a process of decomposition, resulting in the formation of a vitreous phase and crystallization at high temperature. Thus, and according to the temperature reached during the firing, it can be assumed that the phases that crystallize during the firing will be those that form its thermodynamic equilibrium triangle (Heimann, 2010, Maggetti, 1982). Therefore, it can be seen that most of red paste ceramics show a tendency to be non-calcareous (with CaO below 5%), crystallizing in the limit of the manorthite-quartz-mullite and quartz-anorthite-wollastonite equilibrium triangles, while the rest of productions show a tendency to be calcareous (with CaO above 5%, and above 15% in many cases), crystallizing in the quartz-anorthite-wollastonite triangle.

The study of the mineralogical phases of ancient potteries is of high relevance in archaeological sciences because it provides researchers with clues on the thermal history of the ceramic, as well as with unique information about ancient technology and pottery recipes or know-how of the potters and their *chaîne opératoire*. Thus, the thorough understanding of the different mineral phases (primary, neo-formed phases and secondary or contamination) present

or absent in any ceramic paste is a key tool to understand the technical and physicochemical processes involved in the history of any ceramic since it is made, utilized, buried and, eventually found and studied by contemporary researchers. Therefore, knowing the components and features of the ceramic fabrics enables estimating the temperature that a pot was once fired. This approximation is known as equivalent firing temperature (EFT). Besides, mineralogical analysis by XRD also enables to identify secondary or alteration phases (Buxeda et al., 2002). Although other analytical techniques have contributed to the estimation of firing temperatures of ancient ceramics, like Mossbauer (Wagner et al., 2000) magnetic-related techniques (Rasmussen et al., 2012), thermal expansion techniques or SEM (Maniatis and Tite, 1981), just to mention a few, XRD analysis enables a quick, accurate and relatively non-expensive approach to the basic mineral composition of archaeological ceramics.

Table 3 reports identification of main mineral phases after XRD analyses of 32 ceramics from Angra D shipwreck (unfortunately, ANG023 and ANG025 were not analyzed by XRD due to sample size constrains). Mineralogically, Sevillian ascribed ceramics from Angra show typical calcareous earthenware phase associations, similar to the ones already described for the reference groups of Seville (Gomez Ferrer et al., 2013; Iñañez, 2007; Fernández de Marcos et al., 2017). Thus, quartz, plagioclase (mainly albite, but anorthite is present in two samples), diopside and gehlenite, sometimes also calcite (likely of secondary origin), are the main mineral phases, providing an EFT around 950-1000 ºC (Table 3 and Figure 7). However, it is important to highlight the presence of wairakite in some of the Sevillian glazed and tin-lead glazed ceramics, a calcium zeolite [$Ca(Al_2Si_4)O_{12}.2H_2O$]. Wairakite forms a solid solution with analcime [$NaAlSi_2O_6 \cdot H_2O$]. Given the presence of high calcareous ceramics fired at temperatures around or over 1000 ºC, wairakite is suggested as a secondary phase, likely related to the alteration of the vitreous phase of the clay matrix and the posterior crystallization of this zeolite likely as a by-product of gehlenite decomposition under humid conditions (Maggetti and Heinmann, 1981; Maggetti, 1981) (Figure 7). Gypsum ($CaSO_4 \cdot 2H_2O$) is also present in some of the ceramics, especially on the unglazed ones, like the olive jars, as a common secondary precipitation on the outer surface of the ceramics (Figure 7, Table 3).

Finally, red wares (ANG030 and ANG031) show relevant amounts of hematite, main responsible for the reddish color of the ceramic body, quartz and potassium feldspar as main mineralogical phases, along with a likely high amount of vitreous material given the elevation of the background in 25º2Θ (Figure 7, Table 3).

Additionally, framboidal aggregates of Fe and S have been identified by SEM-EDS in some of the transparent green lead glazed and tin-lead glazed ceramics (Figure 8). These framboidal aggregates show a chemical profile consisting on Fe and S, according to EDS microanalyses and are, most likely, pyrite neoformed crystallite. In underwater close harbor conditions, sulphate-reducing microorganisms (SRM) may colonize the ceramic favoring the increase of sulphide concentration in pore-water through a series of reactions from mackinawite (Fe_9S_8) to greigite ($Fe^{2+}Fe^{3+}{}_2S_4$) and, eventually, pyrite (FeS_2) (see Pradell et al., 1996 andSecco et al., 2011 for a thorough discussion). In underwater shipwrecks, abundant organic material might be available and, therefore, higher microbial activity that favored the crystallization of pyrite in these ceramics.

4. Conclusions

Ceramics recovered in Angra D were what could be expected from a context of Spanish origin from the 1st quarter of the 17th century, with clear similarities, at typological point of view, for example, with the collection of *Atocha*, *Santa Margarita* and the unidentified wreck of Tortugas from 1622 (Marken, 1994; Avery, 1997; Stemm et al., 2013). Other types of artefacts provide us with relevant clues regarding the origin of the ship, such as seeds, other vegetal species, coconuts and malacological fauna of tropical origin. The presence of mercury between the timbers of the hull is also a possible evidence of an American origin, as it was intensively used in silver mines explorations. The insects detected on the bow area of the ship were preliminary identified as being from Central America (Bettencourt, 2017, pp. 376-380, 398-400).

Accordingly, ceramics found at the Angra shipwreck site show a Spanish provenance, from Seville, and according to botanical and archaeological

evidences, the ship was returning from the Americas. Moreover, two unglazed red ceramics were identified with Aveiro. Along these lines, this is a group very well known archaeologically in Portugal based on the study of the ship cargo from Ria de Aveiro A shipwreck (Bettencourt and Carvalho, 2008) and, although chemical analyses carried out on samples from various contexts of the north of the country have been carried out (Castro et al., 2003; Sanchez-Garmendia et al., 2019), further studies including the creation of reference groups from production contexts will shed light into this subject.

The olive jars were used to transport goods, namely olive oil and wine, during the trip between Europe, America and Europe. Some of them were used in the round trip from America to Iberian Peninsula during early 17th century as food containers. Regularly, olive jars were sometimes reused in colonial architecture, especially in relation to the vaults of civil and religious buildings. The other ceramics from Seville would be used daily on board. The presence of everyday use Aveiro ceramics, although rarer in Spanish contexts, is also documented in the Tortugas shipwreck (Stemm et al., 2013: 60, Fig. 120).
Consequently, the available information points out that Angra D corresponds to a Spanish ship operating on the Atlantic. It would have commercial functions and, at some stage of its last journey, touched in Central or South America. Its last location should relate with a technical stopover in the Angra port.

In addition, secondary phases found in the ceramics can be related to the close conditions formed on the archaeological context, like the pyrite mineral phases. The reaction into these secondary phases are due to the existence of favorable conditions, which in this case is mainly due to higher reducing conditions due to less water mobility, abundance of organic material and higher microbial activity than in open-sea environments. Besides, wairakite, a calcium zeolite, were also identified in several shards, as well as gypsum and calcite. On the one hand, wairakite is formed as an alteration of the vitreous phase of the high temperatures calcareous ceramics after gehlenite decomposition under humid conditions.

Transdisciplinary studies are needed in order to avoid mistakes. According to the ceramic provenance results, it could have been interpreted as a ship in its way to America from Spain. However, according to the archaeometrical and

archaeological evidence, it is suggested that, in fact, the ship was returning from America towards the Iberian Peninsula. Thus, chemical results of these ceramics alone, without further context and dialogue with archaeological data, would induce a fundamental mistake in the interpretation of the site and the historical implications.

5. Acknowledgments

Authors want to thank the support of Fundação para a Ciância e Tecnologia (Project PTDC/HIS-ARQ/104084/2008),and the Spanish Ministerio de Economía y Competitividad (CERANOR-2 HAR2017-84219-P), Ramón y Cajal Program (RYC-2014-16835), and CHAM Strategic Project (FCSH, Universidade NOVA de Lisboa, Universidade dos Açores) by FCT-Fundação para a Ciência e Tecnologia (UID/HIS/04666/2013). USG thanks the University of the Basque Country (UPV/EHU) for doctoral grant Hiring for Research Training (PIF2017/153). Authors want like to thank Coupled Multispectroscopy Singular Laboratory (LASPEA) from the Advanced Research Facilities (SGIker) of The University of the Basque Country UPV/EHU) for SEM-EDS analysis. The authors also acknowledge The General X-ray Service from SGIker of the University of the Basque Country UPV/EHU, as well as technical and human support provided by the SGIker-Geochronology and Isotope Geochemistry Facility (UPV/EHU, MICINN, GV/EJ, ERDF and ESF). Authors want to thank the valuable comments from two anonymous referees.

6. References

Aitchison, J., 2008. The single principle of compositional data analysis, continuing fallacies, confusions and misunderstandings and some suggested remedies. CoDaWork 2008 1–28.

Aitchison, J., 1986. The Statistical Analysis of Compositional Data. Chapman and Hal, London.

Avery, G., 1997. Pots as Packaging: the Spanish Olive Jar and Andalusian Transatlantic Commercial Activity, 16th-18th Centuries. Phd Thesis submitted to the Florida University.

Bettencourt, 2017. Os naufrágios da baía de Angra (ilha Terceira, Açores): uma

aproximação arqueológica aos navios ibéricos e ao porto de angra nos séculos XVI e XVII, Phd Thesis submitted to Faculdade de Ciências Sociais e Humanas da Universidade Nova de Lisboa, Lisboa.

Bettencourt, J. and Carvalho, P., 2008. A carga do navio Ria de Aveiro A (Ílhavo, Portugal): uma aproximação preliminar ao seu significado histórico-cultural". Cuadernos de Estudios Borjanos. Borja, L-LI, p. 257-287.

Bettencourt, J., Carvalho, P., 2009. Arqueologia marítima na baía de Angra (Angra do Heroísmo, Terceira): enquadramento e resultados preliminares do projecto PIAS, in: AMC - Arqueologia Moderna E Contemporânea. Lisboa, pp. 68–91.

Buxeda i Garrigós, J., 1999. Alteration and Contamination of Archaeological Ceramics: The Perturbation Problem. J. Archaeol. Sci. 26, 295–313.

Buxeda i Garrigós, J., Kilikoglou, V., 2003. Total variation as a measure of variability in chemical data sets, in: van Zelst, L. (Ed.), Patterns and Process. A Festschrift in Honor of Dr. Edward V. Sayre. Smithsonian Center for Materials Research and Education, Suitland, Maryland, pp. 185–198.

Buxeda i Garrigós, J., Madrid i Fernández, M., Iñañez, J., Vila Socias, LL., 2008. Arqueometria ceràmica: una arqueologia ceràmica amb més informació. Cota Zero: revista d'Arqueologia i Ciència, 23, 38–53.

Buxeda i Garrigós, J., Madrid i Fernández, M., Iñañez, J., Fernández de Marcos García, C., 2015. Archaeometry of the Technological change in societies in contact, in: Buxeda i Garrigós, J., Madrid i Fernández, M., Iñañez, J. (Eds.), GlobalPottery 1. Historical Archaeology and Archaeometry for Societies in Contact. Archaeopress, Oxford, pp. 3–26.

Buxeda i Garrigós, J., Mommsen, H., Tsolakidou, A., 2002. Alterations of Na, K and Rb concentrations in Mycenaean pottery and a proposed explanation using X-ray diffraction. Archaeometry 44, 187–198.

Castro, F., Dordio, P. and Teixeira, R., 2003. 200 anos de cerâmica na Casa do Infante (século XVI a meados do século XVIII): identificação visual e química dos fabricos. In 3.as Jornadas de Cerâmica Medieval e Pós-Medieval. Tondela: Câmara Municipal de Tondela, p. 223-230.

Deagan, K.A., 1987. Ceramics, Glassware, and Beads (Artifacts of the Spanish Colonies of Florida and the Caribbean, 1500-1800, volume I. ed.

Smithsonian Institution Press, Washington, D.C.

Fernández de Marcos, C., Buxeda i Garrigós, J., Amores, F., 2017. Nuevos datos sobre la producción de cerámica de cocina y loza basta de Sevilla en los siglos XV-XVI. SPAL. 26, 259-280.

García de Madinabeitia, S., Sánchez Lorda, M.E., Ibarguchi, J.I.G., 2008. Simultaneous determination of major to ultratrace elements in geological samples by fusion-dissolution and inductively coupled plasma mass spectrometry techniques. Anal. Chim. Acta 625, 117–30. doi:10.1016/j.aca.2008.07.024

Garcia, C., Monteiro, P., 2001. The excavation and dismantling of Angra D, a probable Iberian seagoing ship, Angra bay, Terceira Island, Azores, Portugal. Preliminary assessment. Proceedings, Int. Symp. Archaeol. Mediev. Mod. Ships Iberian-Atlantic Tradit. hull Remain. manuscripts, Ethnogr. sources a Comp. approach 431–447.

Garcia, C., Monteiro, P., Phaneuf, E., 1999. Os destroços dos navios Angra C e D descobertos durante a intervenção arqueológica subaquática realizada no quadro do projecto de construção de uma marina na baía de Angra do Heroísmo (Terceira, Açores). Rev. Port. Arqueol. 2, 211–232.

Goggin, J.M., 1960. The Spanish Olive Jar. An indroductory study. Yale Univ. Publ. Antrhopology (Papers Caribb. Anthropol.

Gomez Ferrer, S., Buxeda i Garrigós, J., Garcia Iñañez, J., Amores Carredano, F., Alzate Gallego, A., 2013. Sevillian transport jars in early colonial America: the case of Santa María La Antigua del Darién (Colombia). Open J. Archaeom. 1, 10–15. doi:10.4081/arc.2013.e3

Heimann, R., 2010. Classic and Advanced Ceramics. From Fundamental to Applications. Wiley-VCH, Weinheim.

Iñañez, J.G., 2007. Caracterització arqueomètrica de la ceràmica vidrada decorada de la Baixa Edat Mitjana al Renaixement dels principals centres productors de la Península Ibèrica, 0205107–11th ed. Universitat de Barcelona, Barcelona.

Iñañez, J.G., Buxeda i Garrigós, J., Speakman, R.J., Glascock, M.D., Sosa Suárez, E., 2007. Characterization of 15th-16th Century majolica pottery found on the Canary Islands, in: Archaeological Chemistry: Analytical Techniques and Archaeological Interpretation. pp. 376–398.

Iñañez, J.G., Speakman, R.J., Buxeda i Garrigós, J., Glascock, M.D., 2009. Chemical characterization of tin-lead glazed pottery from the Iberian Peninsula and the Canary Islands: Initial steps toward a better understanding of Spanish Colonial pottery in the Americas. Archaeometry 51, 546–567.

Iñañez, J.G., Speakman, R.J., Buxeda i Garrigós, J., Glascock, M.D., 2008. Chemical characterization of majolica from 14th-18th century production centers on the Iberian Peninsula: a preliminary neutron activation study. J. Archaeol. Sci. 35, 425–440.

Iñañez; J., Bento Torres, J.,; Calparsoro-Forcada, E.; Arana, G., Teixeira, A., 2016. El abastecimiento cerámico de Alcázar Seguer en época portuguesa. Nuevos datos a partir de la Arqueometría. Entre les deux rives du Détroit de Gibraltar: Archéologie de frontières aux 14-16e siècles / En las dos orillas del Estrecho de Gibraltar: Arqueología de fronteras en los siglos XIV-XVI. ArqueoArte, 5, pp. 57 - 74. CHAM-FCSH/UNL-UAç, Lisboa.

Lemoine, C., Picon, M., 1982. La fixation du phosphore par les céramiques lors de leur enfouissements et ses incidences analytiques TT - Phosphorus fixation by ceramics during their burial and analytical consequences. Rev. d'archéométrie 6, 101–112.

Maggetti, M., 1981. Composition of Roman pottery from Lousonna (Switzerland), in: Hughes, M.J. (Ed.), Scientific Studies in Ancient Ceramics, British Museum Occasional Paper. British Museum, London, pp. 33–49.

Maggetti, M., Heinmann, R.B., 1981. Experiments on simulated burial of calcareous Terra Sigillata (mineralogical change). Preliminary results, in: Hughes, M.J. (Ed.), Scientific Studies in Ancient Ceramics. British Museum, London, pp. 163–177.

Maggetti , M., 1982. Phase analysis and its signifi cance for technology and origin , in: J.S. Olin and A.D. Franklin (Eds.), Archaeological Ceramics, Smithsonian Institution , Washington DC, pp. 121 – 133.

Maniatis, Y., Tite, M.S., 1981. Technological examination of Neolithic e Bronze Age pottery from central and southeast Europe and from the Near East. Journal of Archaeological Science, 8, 59-76.

Maritan, L., Mazzoli, C., 2004. Phosphates in archaeological finds: implications

for environmental conditions of burial. Archaeometry, 46, 673-683.

Marken, M., 1994. Pottery from Spanish Shipwrecks 1500-1800. Florida University Press, Gainesville.

Martín-Fernández, J., Buxeda i Garrigós, J., Pawlowsky-Glahn, V., 2015. Logratio Analysis in Archeometry: Principles and Methods, in: Barceló, J.A., Bogdanovic, I. (Eds.), Mathematics and Archaeology, CRC Press, Boca Raton, pp. 178-189.

Meneses, A., 2008. Novas escalas ocasionais e relacionamentos exteriores, in: Leite, J., Matos, A., Meneses, A. (Eds.), História Dos Açores. Dos Descobrimentos Ao Século XX. Instituto Açoriano de Cultura, Angra do Heroísmo, pp. 297–324.

Meneses, A., 2005. A economia e as finanças, in: Matos, A. (Ed.), Colonização Atlântica. Nova História Da Expansão Portuguesa. Editorial Estampa, Lisboa, pp. 331–445.

Oertling, T., 2001. The Concept of the Atlantic Vessel, in: Alves, F.J.S., Rodrigues, P.J.P. (Eds.), International Symposium on Archaeology of Medieval and Modern Ships of Iberian-Atlantic Tradition. Instituto Português de Arqueologia, Lisboa, pp. 233–240.

Pradell, T., Vendrell-Saz, M., Krumbein, W.E., Picon, M., 1996. Altérations de céramiques en milieu marin : les amphores de l'épave romaine de la Madrague de Giens (Var). Rev. d'Archéométrie 20, 47–56. doi:10.3406/arsci.1996.936.

R Core Tema, 2014. R, A language and environment for statistical computing. Vienna: R Foundation for Statistical Computing. http://www.R-project.org/ (accessed 9 March 2020).

Rasmussen, K. L., de la Fuente, G., Bond, A., Korsholm Mathiesen, K., Vera, S., 2012. Pottery firing temperatures a new method for determining the firing temperature of ceramics and burnt clay. Journal of Archaeological Science, 39, 1705-1716.

Sanchez-Garmendia, U., Carvalho, P., Bettencourt, J., Silva, R., Arana, G., Iñañez, J., in press. Submerged and reused: an archaeometric approach to the Early Modern ceramics from Aveiro (Portugal). Journal of Archaeological Science Reports.

Schwedt, A., Mommsen, H., Zacharias, N., Buxeda i Garrigós, J., 2006.

Analcime crystallization and compositional profiles - Comparing approaches to detect post-depositional alterations in archaeological pottery. Archaeometry 48, 237–251.

Secco, M., Maritan, L., Mazzoli, C., Lampronti, G.I., Zorzi, F., Nodari, L., Russo, U., Mattioli, S.P., 2011. Alteration processes of pottery in lagoon-like environments. Archaeometry 53, 809–829. doi:10.1111/j.1475-4754.2010.00571.x

Skibo, J., Schiffer, M.B., 2008. People and Things: a Behavioral Approach to Material Culture. Springer, New York.

Stemm, G.; Gerth, E.; Flow, J.; Guerra-Librero C. e Kingsley, S., 2013.The Deep-Sea Tortugas Shipwreck, Florida: A Spanish-Operated Navio of the 1622 Tierra Firme Fleet". Part 2, the Artifacts, Odyssey Marine Exploration Papers 27. Odyssey Marine Exploration.

Wagner, U., Wagner, F. E., Häusler, W., Shimada, I., 2000. The use of Mossbauer Spectroscopy in studies of archaeological ceramics, in: Creagh, D. C., and Bradley, D. A. (Eds.), Radiation in Art and Archaeometry, Elsevier Science, Amsterdam.

Weigand, P.C., Harbottle, G., Sayre, E.V., 1977. Turquoise sources and source analysis: Mesoamerica and the southwestern U.S.A., in: Earle, T.K., Ericson, J.E. (Eds.), Exchange Systems in Prehistory. Academic Press, New York, NY, pp. 15–34.

Whitney DL, Evans BW., 2010. Abbreviations for names of rock-forming minerals. The American mineralogist. Washington, DC.: Mineralogical Society of America;95(1), 185-187.

FIGURE CAPTIONS

Fig. 1 Angra D geographical location.

Fig. 2 Angra D ceramics: A - olive jars; B-C - tin-lead glazed plain white bowls; D - tin-lead glazed plain white plate; E - Blue on Blue tin-glazed plate.

Fig. 3 Left: Graphical representation of the evenness of the compositional variability of the 34 analyzed ceramics by ICP-MS from Angra D. Right: Graphical representation of the evenness of the compositional variability after excluding some elements for the statistical analysis. (vt= Total variability)

Fig. 4 Principal Component Analysis of unglazed and red ware ceramics from Angra D. Ellipses represent a confidence interval of 90%

Fig. 5 Principal Component Analysis of transparent green lead glazed and tin-lead glazed ceramics from Angra D. Ellipses represent a confidence interval of 90%

Fig. 6. Ternary diagram showing the compositions of SiO2, CaO and Al2O3 of the 86 shards classified by their corresponding typology. An Anorthite, Gh Gehlenite, Mul mullite, Qz quartz and Wo Wollastonite (abbreviations after Whitney and Evans, 2010)

Fig. 7 X-ray diffractograms representing the main chemical groups identified in Angra D ceramic set. From top to bottom: ANG005 (olive jar, SEV-A group); ANG032 (tin-lead glazed, SEV-B); ANG030 (red ware). Estimated equivalent firing temperatures (EFT) according to the defined fabrics from the association of crystalline phases by XRD. Afs=alkaline feldspar; Anl=Analcime Pl=plagioclase; Ab=albite; An=Anorthite; Cal=calcite; Di=diopside; Gh-Ak=gehlenite; Hem=Hematite; Illt=illite; Qz=quartz; Wrk=Wairakite; (abbreviations after Whitney and Evans, 2010).

Fig. 8 False colored Electron Scanning Microscopy microphotograph at 3500X magnification (ANG014) showing framboidal aggregates (golden color). Fe and S are major components according to point EDS microanalysis

TABLE CAPTIONS

Table 1 Chemical concentrations of the 34 ceramics from Angra D according to typology and suggested provenance. All values are expressed as ppm ($\mu g \cdot g^{-1}$) except those expressed as weight % in brackets. The uncertainty of these results is of 10 %

Table 2. Calculated average, standard deviation, maximum and minimum values for the ICP-MS concentrations according to the chemical groups identified. Oxides are expressed in wt % and the rest in ng/g.

Table 3. Summary of the main mineral phases identified by XRD. Afs=alkaline feldspar; Anl=Analcime Pl=plagioclase; Ab=albite; An=Anorthite; Cal=calcite; Di=diopside; Gh-Ak=gehlenite; Hem=Hematite; Illt=illite; Qz=quartz; Wrk=Wairakite; (abbreviations after Whitney and Evans, 2010).

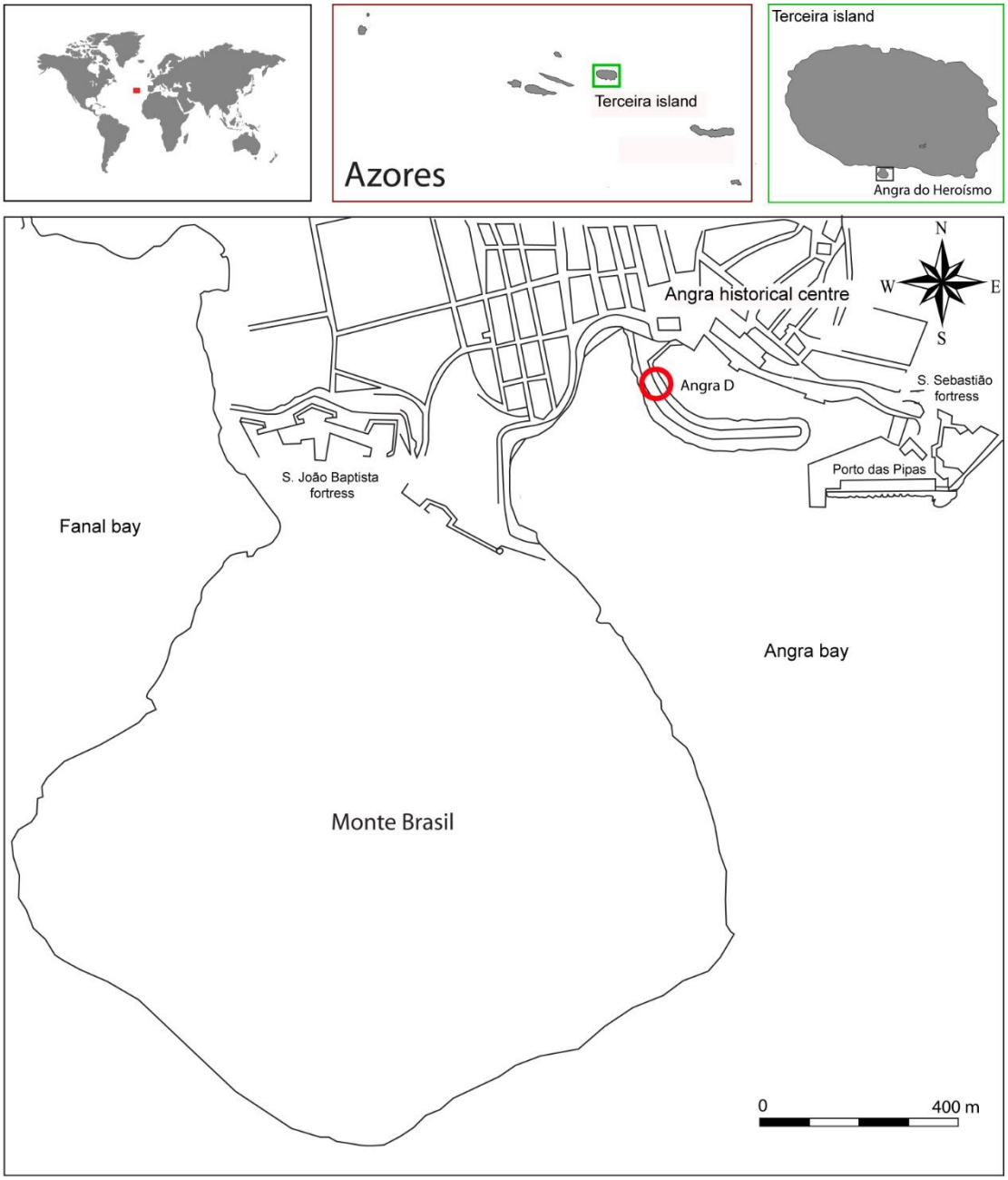
Terceira island
Azores
Terceira island
Angra do Heroísmo
N
W
E
S
Angra historical centre
Angra D
S. Sebastião fortress
Porto das Pipas
S. João Baptista fortress
Fanal bay
Angra bay
Monte Brasil
0
400 m

Fig 1.

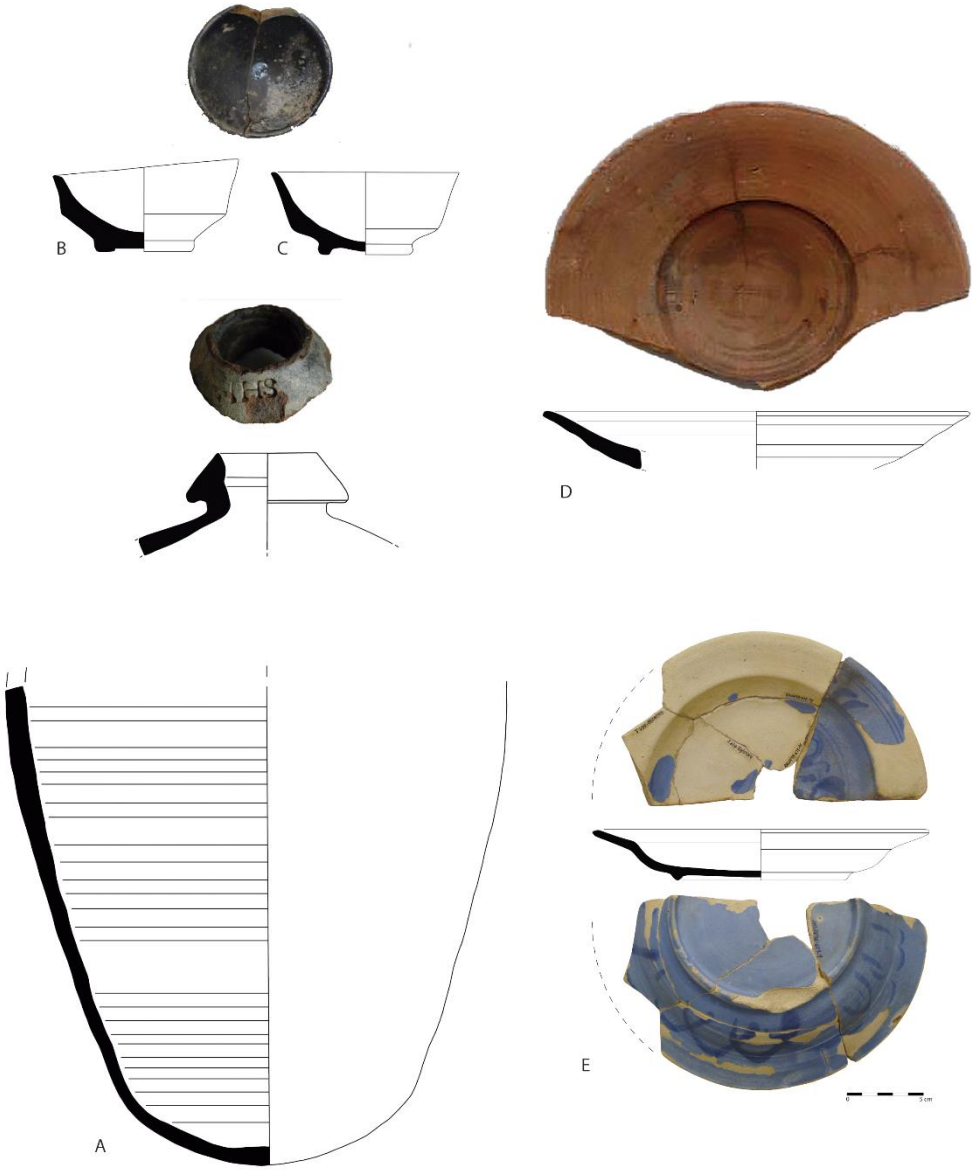

Fig 2.

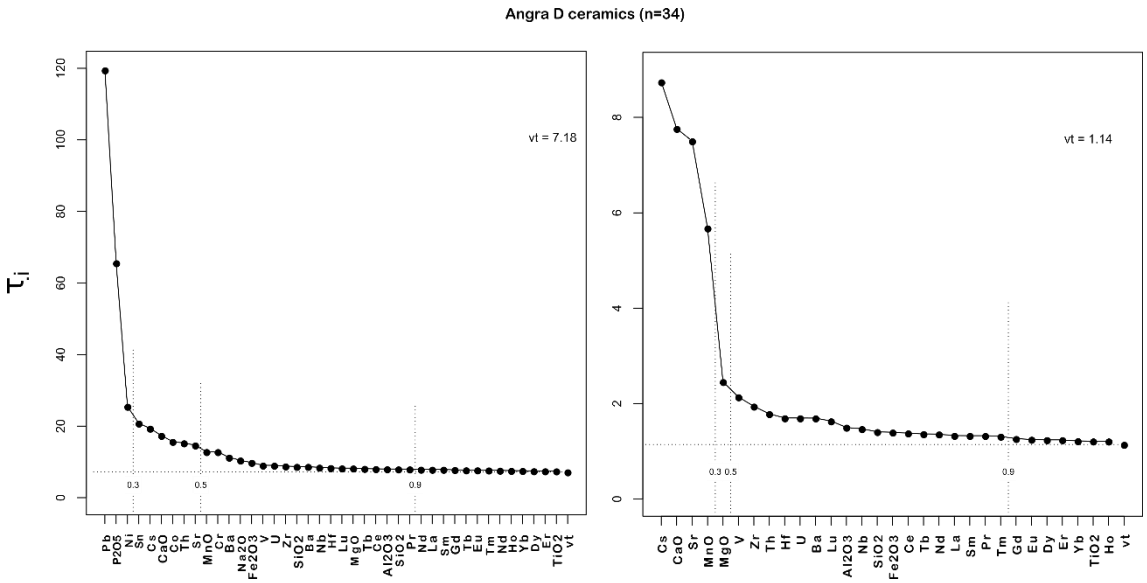
Angra D ceramics (n=34)
vt = 7.18
vt = 1.14
0.3
0.5
0.9
Pb
P2O5
Ni
Sn
Cs
CaO
Cr
Th
Sr
MnO
Cr
Ba
Na2O
Fe2O3
V
U
Zr
SiO2
Ba
Nb
Hf
Lu
MgO
Tb
Ce
Al2O3
SiO2
Pr
Nd
La
Sm
Gd
Tb
Eu
Tm
Nd
Ho
Yb
Dy
Er
TiO2
vt
Cs
CaO
Sr
MnO
MgO
V
Zr
Th
Hf
U
Ba
Lu
Al2O3
Nb
SiO2
Fe2O3
Ce
Tb
Nd
La
Sm
Pr
Tm
Gd
Eu
Dy
Er
Yb
TiO2
Ho
vt

Fig. 3

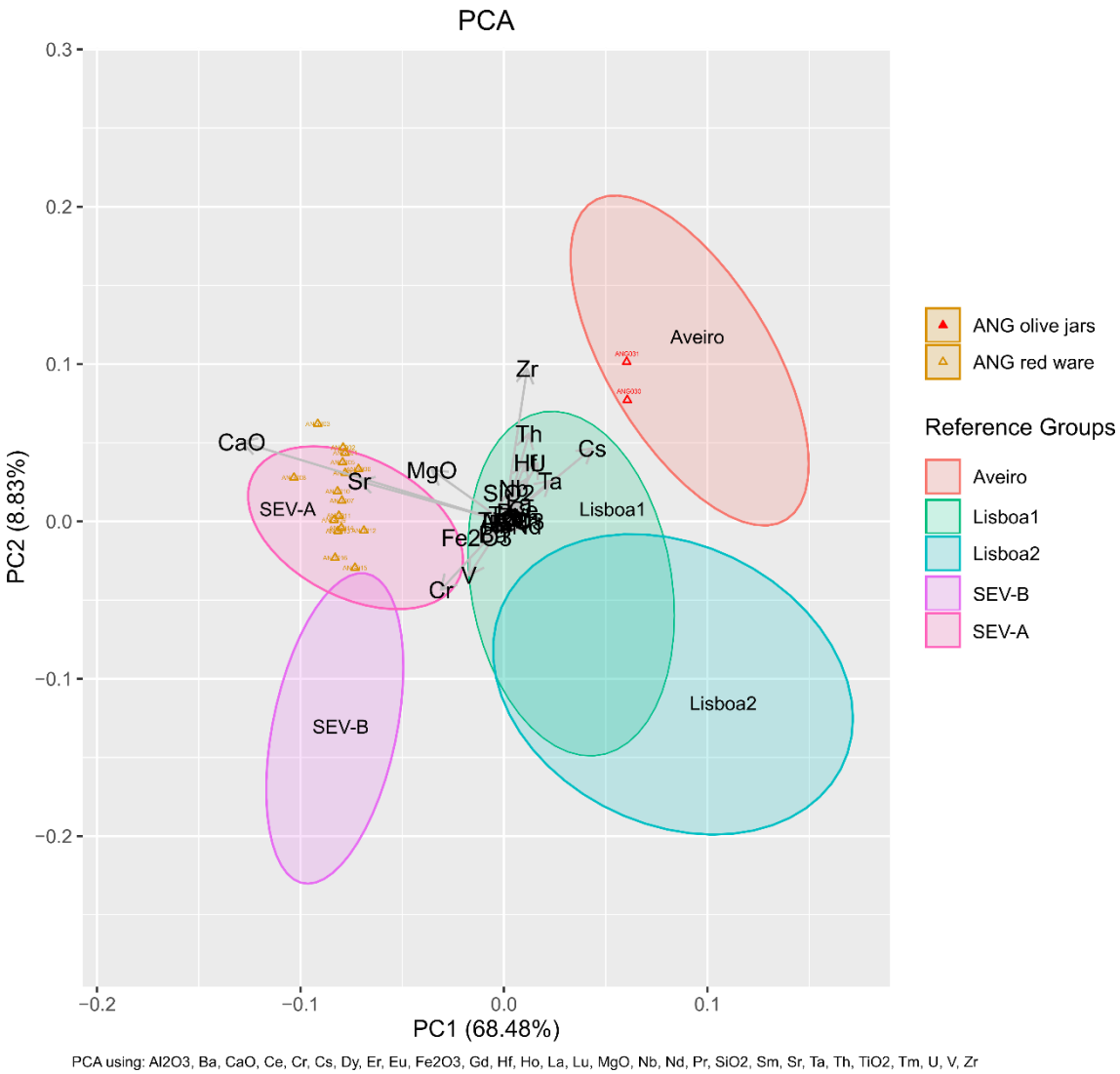

PCA using: Al2O3, Ba, CaO, Ce, Cr, Cs, Dy, Er, Eu, Fe2O3, Gd, Hf, Ho, La, Lu, MgO, Nb, Nd, Pr, SiO2, Sm, Sr, Ta, Th, TiO2, Tm, U, V, Zr

Fig 4.

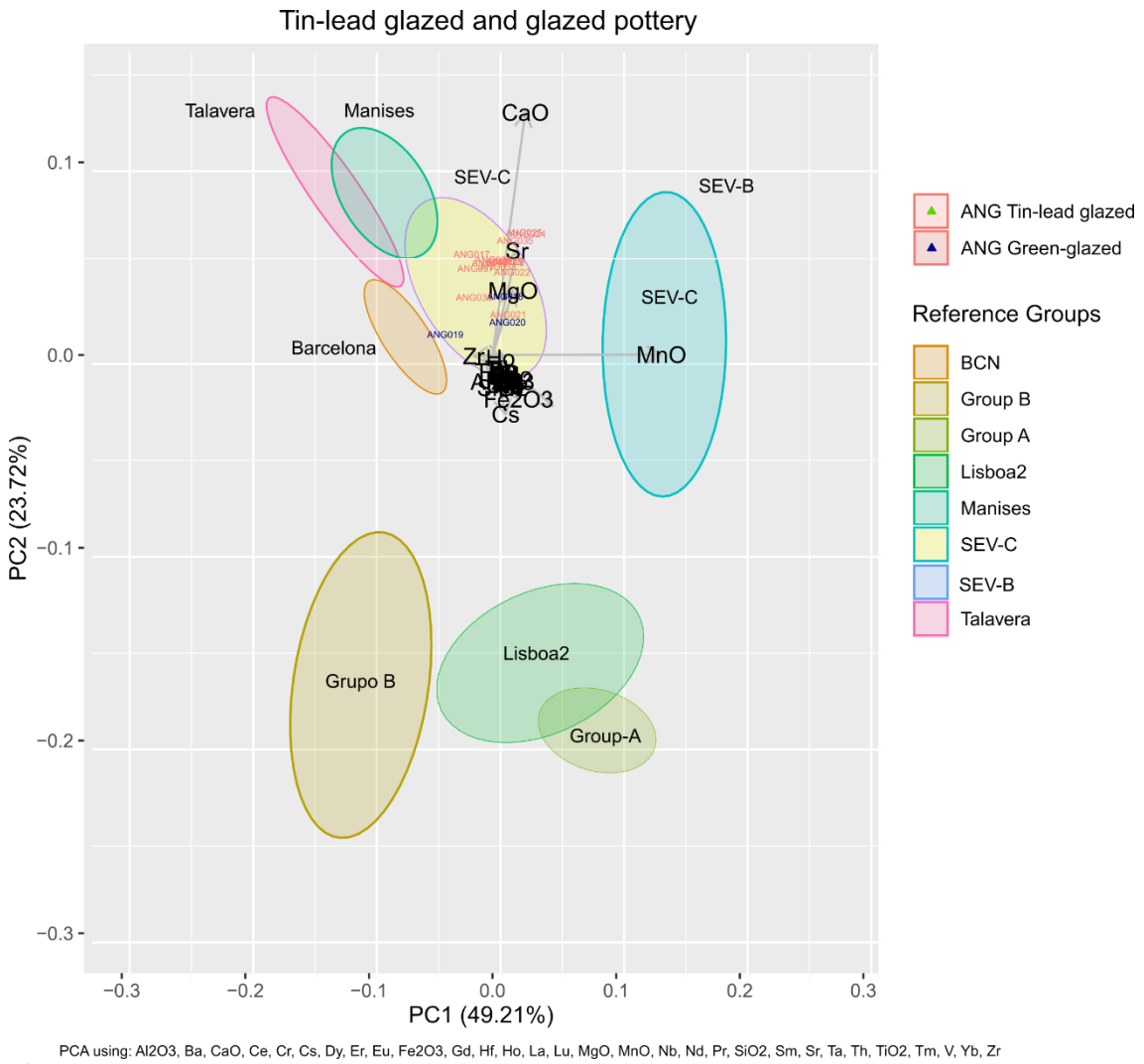

PCA using: Al2O3, Ba, CaO, Ce, Cr, Cs, Dy, Er, Eu, Fe2O3, Gd, Hf, Ho, La, Lu, MgO, MnO, Nb, Nd, Pr, SiO2, Sm, Sr, Ta, Th, TiO2, Tm, V, Yb, Zr

Fig 5.

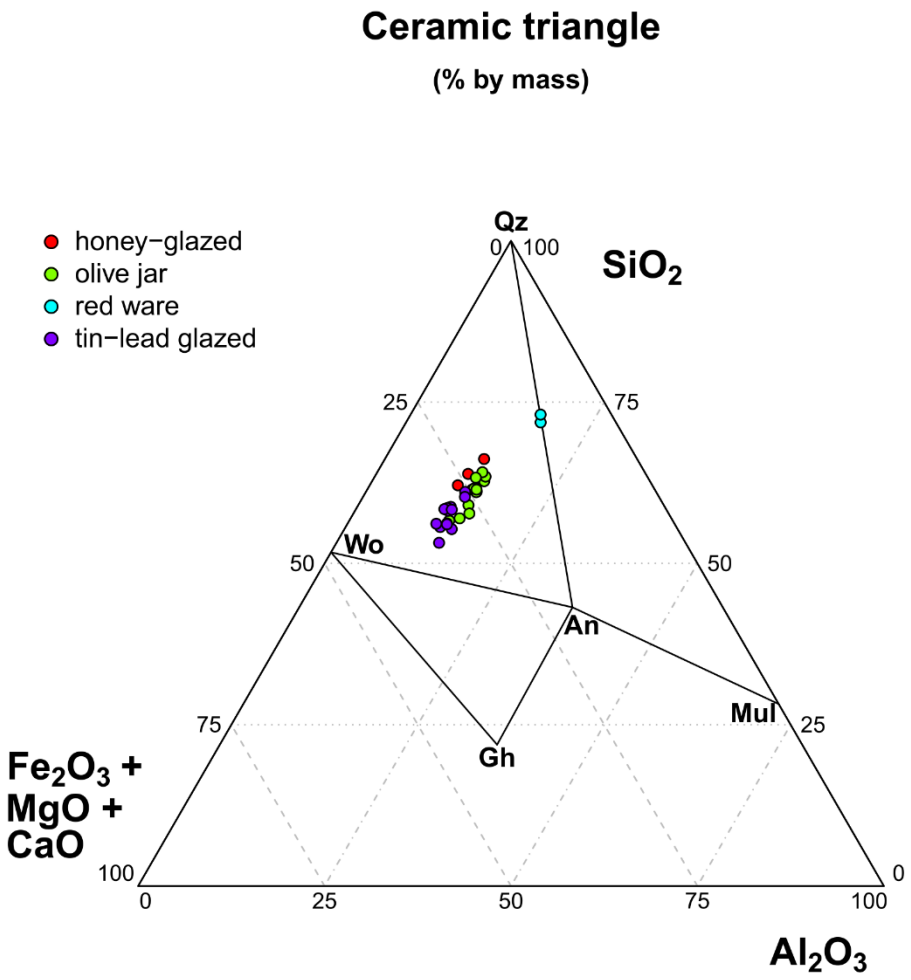
Ceramic triangle
(% by mass)
honey−glazed
olive jar
red ware
tin−lead glazed
Qz
SiO2
Wo
An
Mul
Gh
Fe2O3 +
MgO +
CaO
Al2O3
0
25
50
75
100

Fig 6

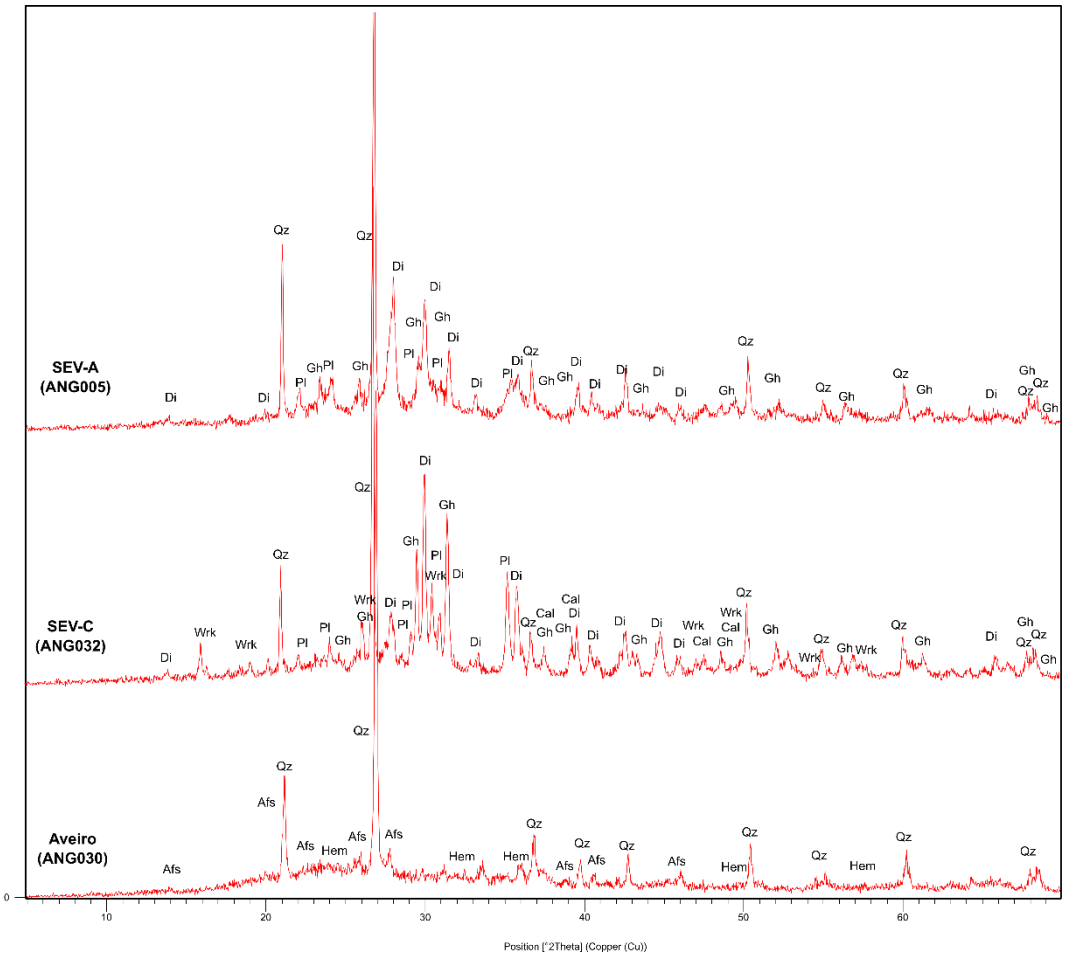
SEV-A
(ANG005)
SEV-C
(ANG032)
Aveiro
(ANG030)
Qz
Di
Gh
Pl
Wrk
Cal
Afs
Hem
0
10
20
30
40
50
60
Position [°2Theta] (Copper (Cu))

Fig 7.

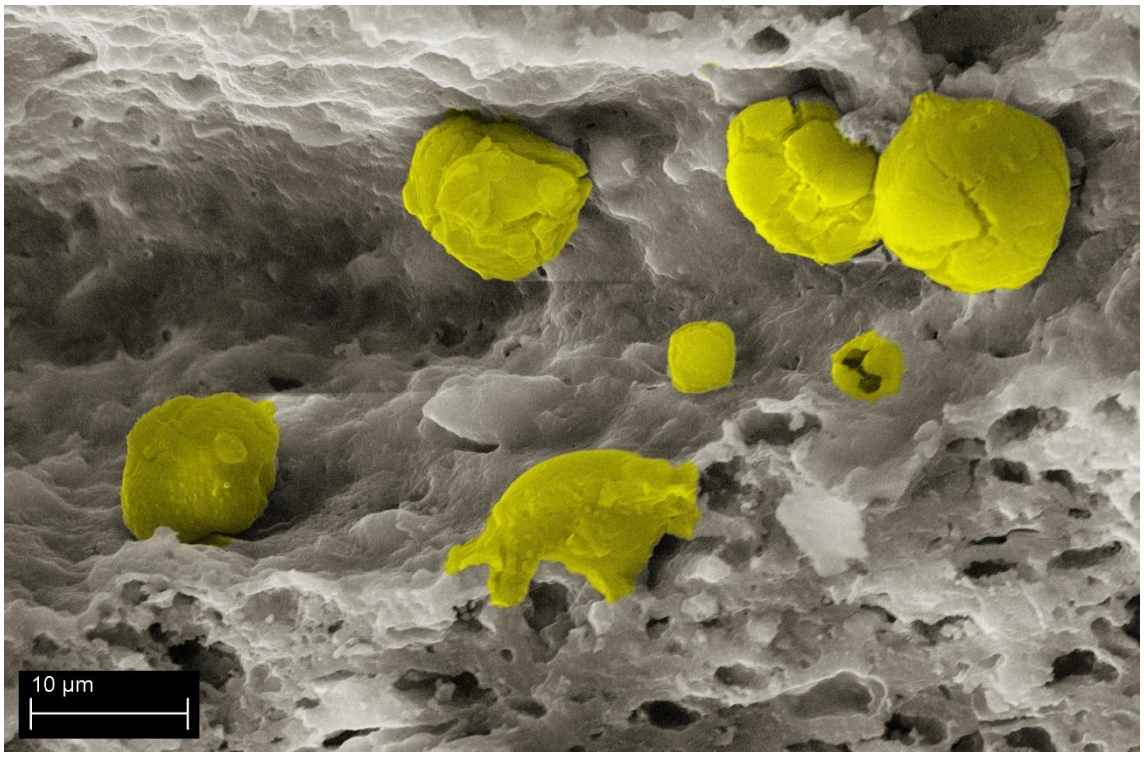

Fig 8

anid	tipology	Provenance	Al2O3	Ba	CaO	Ce	Co
ANG001	olive jar	Sev-A	15.6	545	16.3	79	26.1
ANG002	olive jar	Sev-A	13.8	385	16	71	23.9
ANG003	olive jar	Sev-A	13.6	403	17.8	66	15.5
ANG004	olive jar	Sev-A	13.2	416	14.8	66	20.0
ANG005	olive jar	Sev-A	14.3	434	14.7	69	22.2
ANG006	olive jar	Sev-A	14.2	426	13.2	67	23.0
ANG007	olive jar type B	Sev-A	14.1	443	14.1	69	38.2
ANG008	olive jar	Sev-A	13.3	426	20.4	68	21.2
ANG009	olive jar	Sev-A	13.6	423	14.9	66	25.1
ANG010	olive jar type A "IH" inscription	Sev-A	14	423	15.1	68	25.7
ANG011	olive jar type B	Sev-A	14.1	430	15.1	70	19.7
ANG012	olive jar type A	Sev-A	13.9	402	12.1	68	28.6
ANG013	olive jar type B	Sev-A	13.7	444	14.6	68	18.2
ANG014	olive jar type C	Sev-A	14.2	444	14.3	70	30.4
ANG015	olive jar type B	Sev-A	16.4	510	15	82	61.4
ANG016	olive jar type B	Sev-A	13.5	440	14.3	67	16.6
ANG017	tin lead-glazed blue on white	Sev-C	12.1	327	20.1	71	41.7
ANG018	green glaze ware	Sev-C	11.9	432	17.8	70	26.3
ANG019	green glaze ware	Sev-C	13.2	323	12.6	75	33.9
ANG020	green glaze ware	Sev-C	12.1	435	15.1	70	16.9
ANG021	tin lead-glazed blue on blue	Sev-C	12.9	338	13.9	58	86.9
ANG022	tin lead-glazed blue on blue	Sev-C	12.3	322	17.2	55	103.9
ANG023	tin lead-glazed blue on blue	Sev-C	13.3	438	21.4	74	87.1
ANG024	tin lead-glazed blue on blue	Sev-C	12.7	413	22.8	71	52.1
ANG025	tin lead-glazed blue on blue	Sev-C	13.5	436	23.4	74	90.0
ANG029	tin lead-glazed blue on blue	Sev-C	14.1	451	20.6	78	47.4
ANG030	red ware	Aveiro	18.1	411	2.9	105	39.9

ANG031	red ware	Aveiro	17.5	396	2.5	94	29.3
ANG032	tin lead-glazed white plain	Sev-C	12.6	289	21.3	73	25.6
ANG033	tin lead-glazed white plain	Sev-C	11.5	355	20.5	69	27.9
ANG034	tin lead-glazed white plain	Sev-C	12.9	354	20.4	73	25.7
ANG035	tin lead-glazed white plain	Sev-C	11.4	363	22.5	70	18.9
ANG036	tin lead-glazed white plain	Sev-C	13.7	443	17.7	80	28.5
ANG037	tin lead-glazed white plain	Sev-C	12.7	326	19.2	76	35.2

anid	Cr	Cs	Dy	Er	Eu	Fe2O3	Gd	Hf	Ho	K2O	La	Lu
ANG001	94.0	6.1	5.6	2.8	1.6	6.6	5.5	4.8	0.99	2.9	40	0.38
ANG002	82.0	5.6	4.8	2.4	1.2	5.8	4.9	4	0.79	2.9	36	0.35
ANG003	81.0	5.7	4.5	2.3	1.1	5.5	4.6	3.8	0.81	2.7	34	0.31
ANG004	82.0	5.9	4.4	2.3	1.2	5.8	4.6	3.7	0.79	2.5	34	0.27
ANG005	89.0	5.9	4.5	2.4	1.3	5.8	4.8	3.8	0.78	2.9	35	0.29
ANG006	91.0	6.3	4.5	2.3	1.2	5.8	4.6	3.5	0.85	3.1	34	0.29
ANG007	91.0	6.1	4.7	2.5	1.3	6.1	4.9	3.7	0.83	1.9	35	0.29
ANG008	93.0	5.4	4.8	2.4	1.2	6.1	4.8	3.8	0.83	1.9	34	0.29
ANG009	89.0	6.1	4.5	2.2	1.2	5.9	4.7	3.7	0.76	1.9	34	0.31
ANG010	93.0	5.2	4.6	2.4	1.2	5.7	4.8	3.2	0.79	2.9	34	0.29
ANG011	88.0	6.3	4.7	2.5	1.3	5.8	4.8	3.4	0.89	2	35	0.31
ANG012	104.0	6.0	4.8	2.5	1.3	5.9	4.8	3.5	0.89	2.9	34	0.39
ANG013	86.0	5.7	4.6	2.4	1.3	6.1	4.8	3.6	0.81	2.2	34	0.37
ANG014	87.0	6.1	4.8	2.3	1.3	6.1	4.8	3.4	0.87	2	35	0.4
ANG015	111.0	6.6	5.9	3	1.6	7.3	5.9	3.5	1.03	3.2	41	0.41
ANG016	97.0	5.6	4.4	2.4	1.3	5.9	4.7	3.1	0.84	2.4	34	0.39
ANG017	76.0	5.1	5	2.4	1.2	5.5	5.1	4.5	0.84	0.9	36	0.4
ANG018	94.0	4.8	5	2.6	1.4	5.6	5.1	4.3	0.84	2.5	35	0.4

ANG019	90.0	5.8	5.5	2.9	1.3	5.7	5.5	5.1	0.99	2.1	37	0.49
ANG020	91.0	4.7	5.1	2.5	1.4	5.7	5.3	4.4	0.82	2.4	35	0.4
ANG021	439.0	4.6	4.9	2.4	1.1	6.7	4.7	3.2	0.79	2.2	28	0.39
ANG022	397.0	3.7	4.7	2.5	1	6.5	4.5	2.5	0.76	2.2	27	0.4
ANG023	84.0	4.3	5.4	2.7	1.4	5.8	5.6	4	0.89	1.2	38	0.38
ANG024	77.0	1.9	5.2	2.7	1.3	5.5	5.3	3.7	0.89	1	36	0.38
ANG025	93.0	1.7	5.4	2.9	1.4	5.6	5.4	3.6	0.92	1	37	0.38
ANG029	109.0	3.8	5.8	2.9	1.5	5.8	5.9	3.8	0.93	1.5	39	0.38
ANG030	53.0	26.9	6.4	3	1.5	5.2	7	4.2	0.98	4.4	48	0.36
ANG031	63.0	25.6	5.3	2.6	1.3	5.3	5.8	4.5	0.75	4.1	46	0.35
ANG032	104.0	4.6	5.5	2.9	1.3	5.8	5.4	4.8	0.9	0.9	37	0.34
ANG033	123.0	4.9	5.2	2.8	1.3	5.2	5.4	4.1	0.87	1.3	35	0.36
ANG034	87.0	5.0	5.4	2.8	1.4	5.6	5.4	4.4	0.86	1.3	37	0.36
ANG035	96.0	3.9	5.2	2.8	1.3	5.2	5.2	5	0.85	1.3	35	0.32
ANG036	90.0	5.6	5.6	2.9	1.4	5.6	5.8	5.3	0.9	1.5	40	0.34
ANG037	85.0	5.0	5.5	2.9	1.3	5.9	5.7	5.2	0.89	1	38	0.34

anid	MgO	MnO	Na2O	Nb	Nd	Ni	P2O5	Pb	Pr	Rb	SiO2	Sm
ANG001	2.8	0.09	1.1	17	32.2	18.5	0.2	80	8.8	116	66	6.2
ANG002	2.9	0.08	0.9	15	28.3	15.4	0.1	58	7.8	105	55.9	5.4
ANG003	3.4	0.07	1	15	26.8	14.8	0.1	446	7.2	104	53.8	5.3
ANG004	2.6	0.06	1	14	26.8	16	0.1	90	7.2	102	58.5	5.2
ANG005	2.9	0.07	0.9	15	27.8	13.8	0.1	586	7.7	111	59.8	5.4
ANG006	2.2	0.07	1.1	14	27.3	16.8	0.1	97	7.5	116	60.1	5
ANG007	3	0.07	1.6	14	27.8	15.8	0.1	27	7.6	98	58.9	5.2
ANG008	3.6	0.09	1.5	15	27.5	17	0.1	479	7.3	88	57.1	5
ANG009	2.8	0.07	1.5	13	27.3	15.6	0.1	101	7.3	97	51.2	5.2

ANG010	2.8	0.06	0.9	14	27.1	23.1	0.1	391	7.3	105	61.1	5
ANG011	3	0.06	1.4	15	28.2	16.2	0.1	346	7.6	93	61.4	5.2
ANG012	2.5	0.06	0.9	14	27.6	21.3	0.1	139	7.4	110	60.2	4.9
ANG013	2.8	0.08	1.5	14	27.8	16.2	0.1	333	7.6	98	60.1	5.1
ANG014	3	0.07	1.5	14	27.9	16.6	0.1	27	7.6	101	60.4	5.2
ANG015	3.3	0.1	1.1	19	33.2	21.9	0.2	129	8.8	125	75.7	6
ANG016	2.9	0.08	1.2	15	27.2	16.1	0.1	89	7.3	95	63.6	4.9
ANG017	3.2	0.07	1.2	16	29.1	11.2	0.2	6799	7.8	49	57.3	5.4
ANG018	3.2	0.12	0.9	15	29.8	37.5	0.2	245	7.7	91	63.6	5.3
ANG019	2.3	0.06	0.8	17	31.4	17.9	0.3	348	8.1	95	66.7	5.6
ANG020	2.9	0.1	0.9	15	29.9	22.3	0.2	91	7.6	93	63.8	5.2
ANG021	4.5	0.07	1.7	13	25	208.9	0.1	3383	6.3	94	60.1	4.5
ANG022	4.8	0.07	1.5	12	23.8	196.1	0.1	2549	6	73	58.6	4.5
ANG023	3.6	0.12	1.7	16	31.7	31.5	0.2	1845	8.2	54	57	5.7
ANG024	3.8	0.16	1.5	18	30.4	19	0.1	2608	7.7	32	56.6	5.5
ANG025	3.8	0.13	1.7	16	31.7	20.9	0.2	1873	8	28	53	5.7
ANG029	3.6	0.12	1.3	16	33.6	23.6	0.2	1895	8.4	48	55	5.9
ANG030	2.1	0.03	0.5	22	42.8	5	0.1	33	10.9	291	72.9	7.8
ANG031	1.8	0.02	0.5	22	38.4	4.6	0.1	16	9.7	274	74.2	6.6
ANG032	3.5	0.09	1.3	15	30.7	20.4	0.1	3832	7.8	34	61.6	5.9
ANG033	3.5	0.09	1.3	15	30.1	21.5	0.1	2349	7.5	59	57.6	5.3
ANG034	3.8	0.1	1.3	15	31.7	17.3	0.2	1320	8	64	54.9	5.7
ANG035	3.3	0.17	1.2	15	29.7	16.6	0.2	2069	7.6	51	54.7	5.4
ANG036	3.1	0.07	1.3	16	34	18.7	0.2	2738	8.6	71	61.4	6.5
ANG037	3.6	0.08	1.3	15	33.1	20.7	0.2	4278	8.4	38	58.4	6

anid	Sn	Sr	Ta	Tb	Th	TiO2	Tm	U	V	Yb	Zn	Zr

ANG001	6.1	544	1.6	0.9	11	0.79	0.41	3.1	116	2.7	108	187
ANG002	6.1	414	1.3	0.8	10	0.69	0.32	2.6	99	2.4	92	157
ANG003	6.8	546	1.2	0.7	9	0.63	0.36	3	98	2.3	93	149
ANG004	4.3	425	1.3	0.7	10	0.71	0.4	2.7	98	2.4	85	145
ANG005	7.6	471	1.3	0.7	10	0.7	0.35	2.7	104	2.4	79	141
ANG006	7.3	392	1.3	0.8	10	0.65	0.34	2.9	101	2.3	91	134
ANG007	3	395	1.4	0.7	10	0.68	0.33	2.3	96	2.4	82	144
ANG008	4.8	595	1.3	0.7	9	0.71	0.33	2.7	108	2.4	87	143
ANG009	3.2	414	1.1	0.8	9	0.68	0.34	2.4	103	2.4	79	138
ANG010	4.4	444	1.4	0.7	9	0.66	0.32	2.7	104	2.4	82	136
ANG011	5.6	417	1.3	0.7	10	0.69	0.33	2.8	109	2.5	76	134
ANG012	7.4	364	1.2	0.7	9	0.67	0.4	2.5	103	2.5	77	136
ANG013	5.8	424	1.3	0.7	9	0.66	0.37	2.2	108	2.5	76	141
ANG014	2.8	407	1.2	0.8	10	0.67	0.39	2.4	102	2.5	69	132
ANG015	4.7	511	2	1	11	0.82	0.39	2.6	118	3.1	98	125
ANG016	4.8	446	1.4	0.7	9	0.67	0.37	2.3	108	2.5	70	108
ANG017	233.8	565	1.5	0.8	10	0.67	0.36	2.7	79	2.6	62	158
ANG018	4.4	401	1.5	0.9	9	0.72	0.36	2.5	94	2.7	71	155
ANG019	5.5	326	1.7	1	10	0.75	0.35	3	102	3.1	91	192
ANG020	2.7	378	1.5	0.9	9	0.7	0.34	2.3	87	2.8	75	161
ANG021	98.4	526	1.5	0.8	8	0.69	0.33	2.3	95	2.5	96	109
ANG022	26.1	652	1.5	0.7	8	0.65	0.35	2.2	80	2.4	82	84
ANG023	172.5	620	1.9	0.9	10	0.72	0.35	2.7	94	2.8	94	145
ANG024	39.9	619	1.6	0.8	10	0.68	0.36	2.4	87	2.8	92	144
ANG025	27.3	689	1.7	0.8	10	0.68	0.38	2.4	94	2.9	80	137
ANG029	24	635	1.6	0.9	11	0.72	0.39	2.7	92	2.9	89	142
ANG030	17.8	82	3.6	1	17	0.66	0.39	3.7	57	2.9	46	154
ANG031	23.5	85	3.6	0.9	17	0.66	0.4	4.4	60	2.6	33	168

ANG032	41.9	470	1.4	0.9	11	0.74	0.41	2.6	75	2.7	107	193
ANG033	47.4	544	1.4	0.8	9	0.69	0.43	2.5	80	2.6	75	164
ANG034	43.1	615	1.6	0.8	10	0.67	0.43	2.7	85	2.8	82	176
ANG035	64.6	624	1.3	0.8	9	0.62	0.38	2.6	82	2.8	93	202
ANG036	46.5	487	1.7	0.9	12	0.75	0.41	2.8	78	2.8	113	210
ANG037	59.4	498	1.6	0.9	11	0.72	0.41	2.8	77	2.9	79	209

Table 1.

	SEV-A				SEV-A				ANG030	ANG031
	Mean	std	Min.	Max.	Mean	std	Min.	Max.	conc.	conc.
Al2O3	14.1	0.8	13.2	16.4	12.7	0.8	11.4	14.1	18.1	17.5
Ba	437	39	385	545	378	56	289	451	411	396
CaO	15.2	1.9	12.1	20.4	19.2	3.2	12.6	23.4	2.9	2.5
Ce	70	5	66	82	71	6	55	80	105	94
Co	26.0	11.0	15.5	61.4	46.8	28.7	16.9	103.9	39.9	29.3
Cr	91	8	81	111	133	112	76	439	53.0	63.0
Cs	5.9	0.4	5.2	6.6	4.3	1.1	1.7	5.8	26.9	25.6
Dy	4.8	0.4	4.4	5.9	5.3	0.3	4.7	5.8	6.4	5.3
Er	2.4	0.2	2.2	3.0	2.7	0.2	2.4	2.9	3	2.6
Eu	1.3	0.1	1.1	1.6	1.3	0.1	1	1.5	1.5	1.3
Fe2O3	6.0	0.4	5.5	7.3	5.7	0.4	5.2	6.7	5.2	5.3
Gd	4.9	0.3	4.6	5.9	5.3	0.4	4.5	5.9	7	5.8
Hf	3.7	0.4	3.1	4.8	4.2	0.8	2.5	5.3	4.2	4.5
Ho	0.85	0.07	0.76	1.03	0.87	0.06	0.76	0.99	0.98	0.75
K2O	2.5	0.5	1.9	3.2	1.5	0.6	0.9	2.5	4.4	4.1
La	35	2	34	41	36	4	27	40	48	46
Lu	0.33	0.05	0.27	0.41	0.38	0.04	0.32	0.49	0.36	0.35
MgO	2.9	0.3	2.2	3.6	3.5	0.6	2.3	4.8	2.1	1.8
MnO	0.07	0.01	0.06	0.10	0.10	0.03	0.06	0.17	0.03	0.02
Na2O	1.2	0.3	0.9	1.6	1.3	0.3	0.8	1.7	0.5	0.5
Nb	15	1	13	19	15	1	12	18	22	22
Nd	28.2	1.8	26.8	33.2	30.4	2.7	23.8	34	42.8	38.4
Ni	17.2	2.7	13.8	23.1	44.0	62.2	11.2	208.9	5	4.6
P2O5	0.1	0.03	0.1	0.2	0.2	0.1	0.1	0.3	0.1	0.1
Pb	214	184	27	586	2389	1681	91	6799	33	16
Pr	8	0	7	9	8	1	6	8.6	10.9	9.7

Rb	104	10	88	125	61	23	28	95	291	274
SiO2	60	5	51	76	59	4	53	66.7	72.9	74.2
Sm	5.3	0.4	4.9	6.2	5.5	0.5	4.5	6.5	7.8	6.6
Sn	5	2	3	8	59	62	2.7	233.8	17.8	23.5
Sr	451	65	364	595	541	107	326	689	82	85
Ta	1.4	0.2	1.1	2.0	1.6	0.1	1.3	1.9	3.6	3.6
Tb	0.8	0.1	0.7	1.0	0.9	0.1	0.7	1	1	0.9
Th	10	1	9	11	10	1	8	12	17	17
TiO2	0.7	0.05	0.6	0.8	0.7	0.04	0.62	0.75	0.66	0.66
Tm	0.4	0.0	0.3	0.4	0.4	0.03	0.33	0.43	0.39	0.4
U	2.6	0.3	2.2	3.1	2.6	0.2	2.2	3	3.7	4.4
V	105	6	96	118	86	8	75	102	57	60
Yb	2.5	0.2	2.3	3.1	2.8	0.2	2.4	3.1	2.9	2.6
Zn	84	10	69	108	86	13	62	113	46	33
Zr	141	16	108	187	161	35	84	210	154	168

Table 2

ANID	tipology	Provenance	EFT (ºC)	Qz	Pl	Gh	Di	Cal	Wair-Analc	Otros Min
ANG001	olive jar	Sev-A	950	x	Ab	x	x	-	-	-
ANG002	olive jar	Sev-A	800-850	x	-	-	-	x	-	Ilt
ANG003	olive jar	Sev-A	900-950	x	Ab	¿?	x	-	-	-
ANG004	olive jar	Sev-A	950	x	Ab	-	x	-	-	-
ANG005	olive jar	Sev-A	950	x	Ab	x	x	-	-	-
ANG006	olive jar	Sev-A	950	x	Ab	x	x	-	-	-
ANG007	botija type B	Sev-A	1000-1050	x	Ab	-	x	-	Wrk	-
ANG008	olive jar	Sev-A	1000-1050	x	Ab	-	x	-	Wrk	-
ANG009	olive jar	Sev-A	1000-1050	x	Ab	-	x	-	Wrk	-
ANG010	olive jar type A "IH" inscription	Sev-A	900-950	x	Ab	¿?	x	-	-	-
ANG011	olive jar type B	Sev-A	1000-1050	x	Ab	-	x	-	Wrk	-
ANG012	olive jar type A	Sev-A	900-950	x	Ab	¿?	x	-	-	-
ANG013	olive jar type B	Sev-A	1000-1050	x	An	-	x	-	Wrk	-
ANG014	olive jar type C	Sev-A	1000-1050	x	An	-	x	-	Wrk	-
ANG015	olive jar type B	Sev-A	900-950	x	Ab	¿?	x	-	-	-
ANG016	olive jar type B	Sev-A	950	x	Ab	-	x	-	-	-
ANG017	tin lead-glazed blue on white	Sev-C	1000-1050	x	Ab	x	x	-	Anl	-
ANG018	green glaze ware	Sev-C	900-950	x	Ab	x	x	x	-	-
ANG019	green glaze ware	Sev-C	950	x	Ab	-	x	-	-	-
ANG020	green glaze ware	Sev-C	900-950	x	Ab	x	x	x	-	-
ANG021	tin lead-glazed blue on blue	Sev-C	950	x	Ab	-	x	-	-	-
ANG022	tin lead-glazed blue on blue	Sev-C	900-950	x	Ab	-	x	-	-	-
ANG024	tin lead-glazed blue on blue	Sev-C	950	x	Ab	x	x	-	-	-
ANG029	tin lead-glazed blue on blue	Sev-C	950	x	Ab	x	x	-	-	-
ANG030	red ware	Aveiro	850-900	x	-	-	-	-	-	Hem, Afs
ANG031	red ware	Aveiro	850-900	x	-	-	-	-	-	Hem, Afs
ANG032	tin lead-glazed white plain	Sev-C	1000-1050	x	Ab	x	x	x	Wrk	-

ANG033	tin lead-glazed white plain	Sev-C	950	x	Ab	x	x	-	-	-
ANG034	tin lead-glazed white plain	Sev-C	1000	x	Ab	x	x	-	¿?	-
ANG035	tin lead-glazed white plain	Sev-C	1000-1050	x	An	x	x	-	Wrk	-
ANG036	tin lead-glazed white plain	Sev-C	1000-1050	x	An	x	x	-	Wrk	-
ANG037	tin lead-glazed white plain	Sev-C	1000-1050	x	Ab	x	x	-	Wrk	-

Table 3.